

## A new mass determination of an eclipsing binary V2080 Cygni<sup>1</sup>

W. Dimitrov<sup>1</sup>, K. Kamiński<sup>1</sup>, K. Bąkowska<sup>2</sup>,  
M. K. Kamińska<sup>1</sup>, J. Tokarek<sup>1</sup>, M. Pawłowski<sup>1</sup>, P. Bartczak<sup>1</sup>  
T. Kwiatkowski<sup>1</sup>, A. Schwarzenberg–Czerney<sup>3</sup>

<sup>1</sup>Astronomical Observatory Institute, Faculty of Physics,  
Adam Mickiewicz University, ul. Słoneczna 36, 60-286 Poznań, Poland  
e-mail: dimitrov@amu.edu.pl

<sup>2</sup>Institute of Astronomy, Faculty of Physics, Astronomy and Informatics,  
Nicolaus Copernicus University, ul. Grudziądzka 5, 87-100 Toruń, Poland

<sup>3</sup>Nicolaus Copernicus Astronomical Center, ul. Bartycka 18, 00-716 Warsaw, Poland

*Received January 30, 2021*

### ABSTRACT

We present a new spectroscopic measurements of the eclipsing binary V2080 Cygni. It is a detached system with a similar components and periode of 4.9 d. We collected data with two instruments, 1.88 m DDO telescope equipped with Cassegrain spectrograph and 0.5 m PST1 connected to a fiber fed echellé spectrograph. We collected 127 measurements for each component, which significantly increase the number of available radial velocity measurements. The obtained masses of the eclipsing components are  $M_1 = 1.190 \pm 0.006$  and  $M_2 = 1.139 \pm 0.005 M_\odot$ . We compared our two data sets with the results of three other investigations. We checked also the influence of the usage of different measurement technics: the cross correlation and broadening function method. We found that the obtained masses depends on the used instrument or measurement technique in about 1-2%, i.e. this is the level of the systematic errors that we could expect. Additionally we analysed the GAIA mission results. The V2080 Cygni A has a three visual companions, however according to GAIA parallaxes and proper motions they cannot be dynamically connected with the eclipsing binary and they are background stars. **The possible existence of third body in the system could be cause of light time effect. We collected a multicolor photometry and calculated a new times of minima. The  $O-C$  diagrams reveal some variations in the orbital period however more data is needed.**

**Key words:** Stars: individual: V2080 Cygni - binaries: eclipsing

### 1. Introduction

Detached eclipsing binaries provide precise determination of stellar radii and masses. The modern photometric and spectroscopic observations allow us to reach

---

<sup>1</sup>Based on the spectroscopic data obtained with Poznań Spectroscopic Telescope 1 and David Dunlap Observatory 1.88 m telescope.

accuracy of about 1% or better for those absolute parameters. The investigated star V2080 Cygni is a relatively bright F5 eclipsing binary with a visual magnitude of 7.4. Other designations of the object are HD 183361 and BD+49 3012. The object is listed as a visually multiple star in Catalog of the Components of Double and Multiple Stars (CCDM; Dommagnet & Nys 1994) and Washington Double Star Catalog (WDS; Mason et al. 2001). The eclipsing nature of the main A star was detected by Hipparcos satellite mission. The light curve has flat maxima and minima with comparable depth as we can expect for similar almost spherical components. The object is a relatively bright and close, i.e. it is a good candidate for precise determination of the absolute parameters. Additionally, the spectral lines of both components are clearly seen. First radial velocity measurements were presented in a short IBVS paper (Kurpínska-Winiarska et al. 2000). Authors yield the amplitudes of the radial velocity curves. They corrected the period of the star, which is twice as long as the one given by Hipparcos. Later two teams observe the star spectroscopically. First group collected thirteen spectra at TUBITAK National Observatory and Catania Astrophysical Observatory (İbanođlu et al. 2008). The velocities were measured with the cross-correlation method. The authors observe the star also photometrically and acquired UBV light curves. They obtained a model of the system using the Wilson-Devinney method. Authors mentioned the existence of third light in the system of about 3%. The second team obtained 8 spectra with ELODIE spectrograph (Aliçavuş et al. 2019). For analysis they used spectral disentangling method. Atmospheric parameters were obtained as well. For modelling of the star authors used also earlier radial velocity measurements of the first team and SuperWASP light curve. Authors detected third light of about 8% in both light curve modelling and spectrum disentangling. The results for masses of both studies agrees within errors. The mass ratio is close to 1 and the obtained masses are  $1.197 \pm 0.005$  and  $1.173 \pm 0.004 M_{\odot}$ . Our spectroscopic observations complement the existing data and increase the number of all available observations in about four times.

## 2. Visual companions

As we mentioned in the introduction V2080 Cyg A have a three bright visual companions. They are listed in WDS and CCDM catalogs of visual doubles. The latest results coming from GAIA mission<sup>2</sup> yield the parallaxes and the proper motions of all four components (Gaia Collaboration et al. 2016; Lindgren et al. 2016). The GAIA DR2 results are presented in Table 1. Both DR1 and DR2 results are in good agreement and show that the all components have different parallaxes and proper motions and they are not connected dynamically. The fainter stars in the close neighbourhood seems to be also a background stars, their proper motions and parallaxes are small (Fig. 1).

---

<sup>2</sup><https://gea.esac.esa.int/archive/>

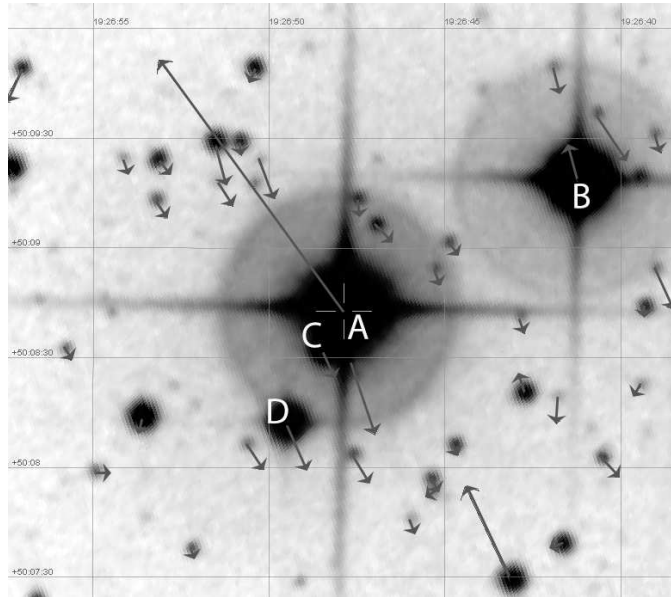


Fig. 1. Proper motions of the V2080 Cyg A neighbourhood stars (GAIA DR2).

Table 1

Proper motions and parallax for V2080 Cyg A and the potential companions from GAIA DR2.

comp. WDS	phot. g (mag)	sep. (arcsec)	$\mu_{\alpha}$ (mas/yr)	$\mu_{\delta}$ (mas/yr)	parallax (mas)
A	7.24	-	$55.50 \pm 0.07$	$75.01 \pm 0.07$	$11.70 \pm 0.03$
C	14.08	14	$-2.97 \pm 0.04$	$-5.94 \pm 0.04$	$0.48 \pm 0.03$
D	11.49	36	$-6.21 \pm 0.06$	$-13.51 \pm 0.05$	$0.57 \pm 0.03$
B	8.57	73	$2.36 \pm 0.13$	$10.41 \pm 0.11$	$2.55 \pm 0.05$

### 3. Spectroscopy and measurements

We have two datasets obtained on a different instruments. So we can compare results of both telescopes as well as with the data from the literature.

First data set was obtained with 1.88 m telescope of the David Dunlap Observatory with the Cassegrain spectrograph between 21st of April and 10th of November 2006. Two different detectors were used 1024x1024 Thomson CCD and later 2048x512 Jobin Yvon Horiba CCD. The exposure times were 1200 s, and we observed the Mg spectral region near 5184 Å. The typical signal-to-noise ratio was in the range of 100 – 150. Data reduction was carried out using a standard IRAF tasks.

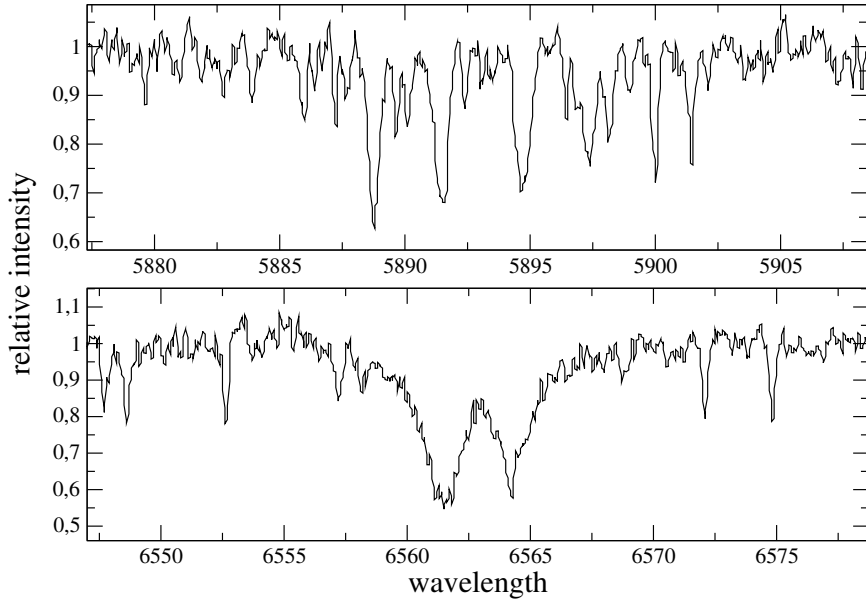


Fig. 2. Two spectral regions of the PST 1 spectrum near NaD and  $H_{\alpha}$  lines.

The second dataset was acquired on 0.5 m Poznan Spectroscopic Telescope (PST1) in the period from 16th of June till 14th of October 2007. The instrument is smaller than the previous one but its connected via fiber to an Echellé spectrograph (Baranowski et al. 2009). The system have very small light losses as the telescope parameters fit perfectly the fiber requirements. The spectrograph is equipped with Andor DZ 436 CCD with 5 stage peltier plus liquide cooling. The spectral range was 4500 - 9200 Å with dispersion of 0.11 Å/pix. The exposure times were 1200 or 1800 s and the typical signal-to-noise ratio is between 25–125. Two spectral regions are presented on the Fig 2. The split spectral lines of both components are clearly seen.

We searched for traces of the third star, mentioned by the previous authors, in the cross correlation function. To enhance the sign of this component we used a low temperature templates. We did not found any significant traces (Fig 3.).

For the radial velocity measurements we have used Broadening Function<sup>3</sup> (BF) method and for comparison and tests we used also the Cross Correlation (CCF) method. Broadening Function was firstly described by S. Rucinski (1992, 2002). The method is resistant to the spectral line broadening and have higher resolution comparing to CCF. The typical BF is presented on the Figure 4. The Cross Correlation measurements was carried out with IRAF task FXCOR.

<sup>3</sup><http://www.astro.utoronto.ca/rucinski/SVDcookbook.html>

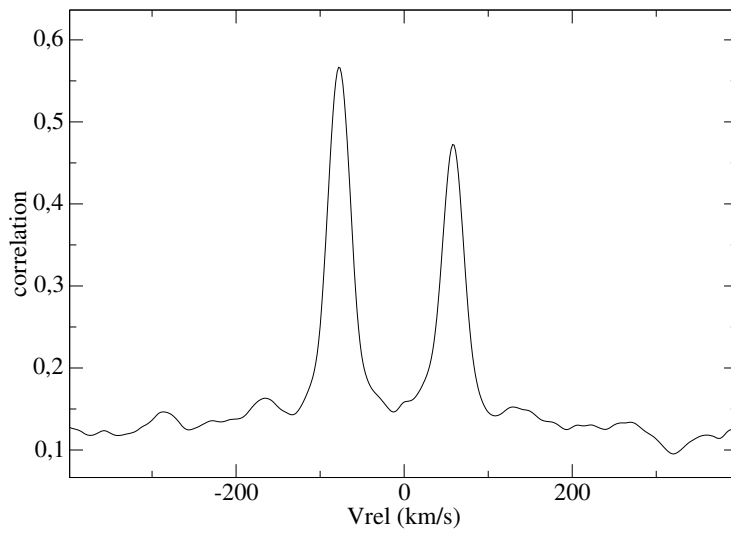


Fig. 3. Cross correlation function for PST 1 spectrum.

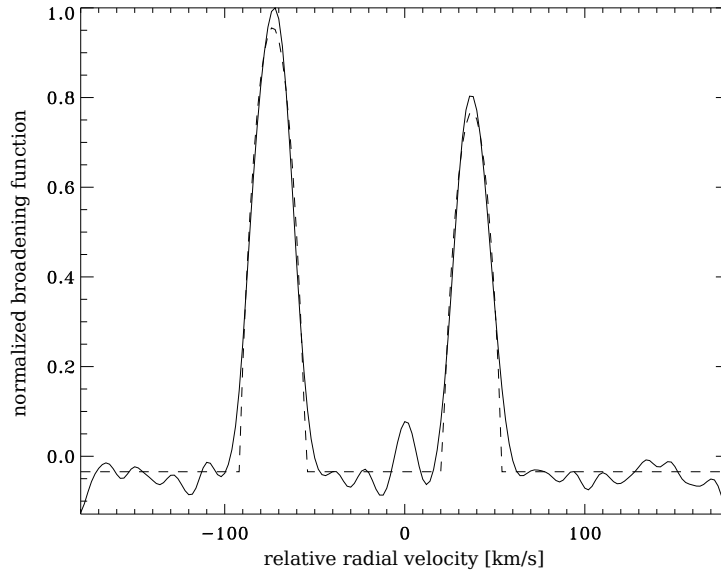


Fig. 4. Broadening function for one of the our PST1 spectra. The solid line present the BF and the dashed line the fitted rotational profiles. The BF is normalized to one and on the horizontal axis we have the relative velocity. The third peak is connected probably with the telluric lines.

#### 4. Mass determination

For the fitting of the radial velocity curves we have employed the PHOEBE SVN code (Prša & Zwitter 2005). The program is based on the Wilson-Devinney method (Wilson & Devinney 1971). As the results of the previous investigations suggests that the eclipsing pair could have a companion we fit the two data sets separately. For our fit we used a period of 4.933588(28) d given by İbanoğlu et al. (2008) and surface potentials and inclination presented by Aliçavuş et al. (2019). We fitted four parameters: semi-major axis, mass ratio, systemic velocity and  $HJD_0$ . The  $HJD_0$  was selected in the middle of the time span of RV observations. As there is a potential third body in the system we could expect light time effect and possible phase shifts with respect to the ephemeris. That was the reason to leave this parameter free. The systemic velocity show some variation that are slightly higher than we could expect from the zero point shifts in different spectrographs. It could be also explained with the existence of third body and motion on the wide orbit.

First two columns of Table 2 present the influence of the usage of different instruments on the obtained results. In both cases Broadening Function method was used for the measurements. We compared the 1.88 m DDO telescope equipped with cassegrain spectrograph and the 0.5 m PST1 telescope with a fiber fed echelle spectrograph. The signal-to-noise ratio of the DDO spectra is higher but the PST1 echelle has wider spectral range. The dispersion of the RV measurements for the PST1 is smaller as we can expect for the spectrograph mounted in a thermally stabilized room. The measured semi-major axis is in very good agreement but the mass ratio differs in about 1%, which propagates in to a 1% differences in masses.

The second and third columns of Table 2 show the same PST1 dataset measured with two methods – BF and CCF. The mass ratio is in very good agreement but the semi-major axis is slightly lower for the CCF results and that causes less than 1% lower masses.

The modern radial velocity measurements yields mass measurements of eclipsing binaries with precision less than 1%, however as we see in the Table 2 and 3 results, masses could differ in about 1-2% depending on the used instrument or measurement method. Usually the listed errors of the obtained parameters are based on the dispersion of the RV/LC measurements and are not taking in to account the possible systematic errors.

##### 4.1. Simultaneous fit

In this section we present the simultaneous fit for all our data. To achieve this we shifted up first data set in  $1.1 \text{ km s}^{-1}$ . This is the difference between the systemic velocities for both data sets. We compared the results with three other investigations (Table 3). Most of the results are in good agreement, only the systemic velocity vary significantly. The masses for our result was calculated for inclination  $86.009^\circ$  yielded by Aliçavuş et al. (2019). The İbanoğlu et al. (2008) results were

Table 2

Fitting results based on our spectroscopic observations.

Instrument Method	DDO BF	PST1 BF	PST1 CCF
$a$ ( $R_{\odot}$ )	$16.16 \pm 0.02$	$16.15 \pm 0.02$	$16.12 \pm 0.02$
$q$	$0.953 \pm 0.003$	$0.965 \pm 0.002$	$0.964 \pm 0.002$
$V_{\gamma}$ ( $\text{km s}^{-1}$ )	$1.76 \pm 0.09$	$2.86 \pm 0.06$	$2.65 \pm 0.06$
$HJD_0 - 2450000$	$3944.7883$ $\pm 0.0012$	$4329.6078$ $\pm 0.0008$	$4329.6072$ $\pm 0.0008$
$M_1$ ( $M_{\odot}$ )	$1.193 \pm 0.006$	$1.183 \pm 0.006$	$1.177 \pm 0.006$
$M_2$ ( $M_{\odot}$ )	$1.137 \pm 0.006$	$1.142 \pm 0.005$	$1.135 \pm 0.005$
$\sigma_{RV}$ ( $\text{km s}^{-1}$ )	1.08	0.59	0.57
$n_{obs}$	80	47	47

calculated for inclination of  $86^{\circ}20$  which is very close to upper one therefore the results could be directly compared without recalculation of semi-major axes and masses. The earliest paper Kurpińska-Winiarska et al. 2000 did not present neither inclination nor semi-major axis values. The error bars were not presented as well. To compare those results with the newer papers we calculated rest of the values using  $i = 86^{\circ}009$ .

All our fitted moments of main eclipse or  $HJD_0$  (Table 2 and 3) were fitted for our RV data for the middle of the period of observation for each data set. The  $HJD_0$  given by Kurpińska-Winiarska et al. (2000) is based on their radial velocity and photometric observations (Tab. 3). In case of the İbanoğlu et al. 2008 result listed in Table 3, the  $HJD_0$  value present their best observed moment of the eclipse. The latest paper K. Aliçavuş & Aliçavuş (2019) present a value based on their RV data.

We collected four times more measurements than all the previous investigations together. Our primary mass value is close to the one obtained by İbanoğlu et al. 2008 while the secondary is about 2% lower. Mases obtained by Aliçavuş et al. (2019) are the highest among all results. While our result yields the lowest value of the mass ratio of the eclipsing pair.

If we compare the error bars of our and Aliçavuş et al. 2019 results listed in Table 3, we could mention that the authors have slightly smaller estimations of the errors. It is surprising because the quality of the RV data is comparable but we have six times more spectra. One significant difference between our and Aliçavuş et al. 2019 results is that we fitted only RV data and they made a simultaneous fit of RV and LC data. We performed the one of the bootstrap method variants to check our error estimations. We randomly draw  $N$  measurements from  $N$  observations with

Table 3  
Comparison of the results

	Kurpińska-Winiarska et al. 2000	İbanoğlu et al. 2008	K. Aliçavuş & Aliçavuş 2019	PST1 & DDO (this paper)	bootst. err.
$a$ ( $R_{\odot}$ )	16.16	$16.20 \pm 0.07$	$16.254 \pm 0.019$	$16.16 \pm 0.02$	0.026
$q$	0.974	$0.971 \pm 0.009$	$0.982 \pm 0.002$	$0.957 \pm 0.002$	0.002
$V_{\gamma}$ ( $\text{km s}^{-1}$ )	3.2	$1.0 \pm 0.4$	$1.17 \pm 0.32$	$2.88 \pm 0.06$	0.08
$HJD_0$ -2450000	1053.705 $\pm 0.001$	3895.4534 $\pm 0.0008$	2504.186 -	4117.4638 $\pm 0.0009$	0.0011
$M_1$ ( $M_{\odot}$ )	1.180	$1.191 \pm 0.017$	$1.197 \pm 0.005$	$1.190 \pm 0.006$	0.007
$M_2$ ( $M_{\odot}$ )	1.149	$1.157 \pm 0.017$	$1.173 \pm 0.004$	$1.139 \pm 0.005$	0.007
$n_{obs}$ method	11 -	13 CCF	21 CCF	127 BF	

possible value repetitions. This way we obtained ten data sets for both components, and we fit the  $RV_{12}$  curves. We calculated the standard deviation of obtained values of the parameters. Our formal errors listed in one before last column of Table 3 are in good agreement and slightly lower than the bootstrap errors listed in the last column.

## 5. Photometry

### 5.1. Observations and data reduction

Observations of V2080 Cyg were obtained during 41 nights from 2009 September 7 to 2011 October 1 at the Poznań Astronomical Observatory located in Poland. For observations we used a 200 mm, F/4.5 Newton reflector, equipped with a SBIG ST-7 XME camera and a set of Bessel BVRI filters. The camera provided a  $17.0' \times 25.5'$  field of view.

All observations were carried out in the V, I and R filters with the exposure times 10, 8, and 6 seconds, respectively. In total, we gathered 108.59 hours and obtained 50699 exposures of V2080 Cyg. Table 4 presents a full journal of our CCD observations.

We determined relative unfiltered magnitudes of V2080 Cyg by taking the difference between the magnitude of the object and the mean magnitude of the three comparison stars. In Fig. 6 the map of a region is displayed with V2080 Cyg marked as V1 and the comparison stars as C1, C2 and C3, respectively. The equatorial coordinates and the brightness of comparison stars C1 (RA =  $19^h 26^m 41^s .246$ , Dec =  $+50^{\circ} 09' 18'' .274$ , 8.56 mag in V filter), C2 (RA =  $19^h 27^m 00^s .870$ ,



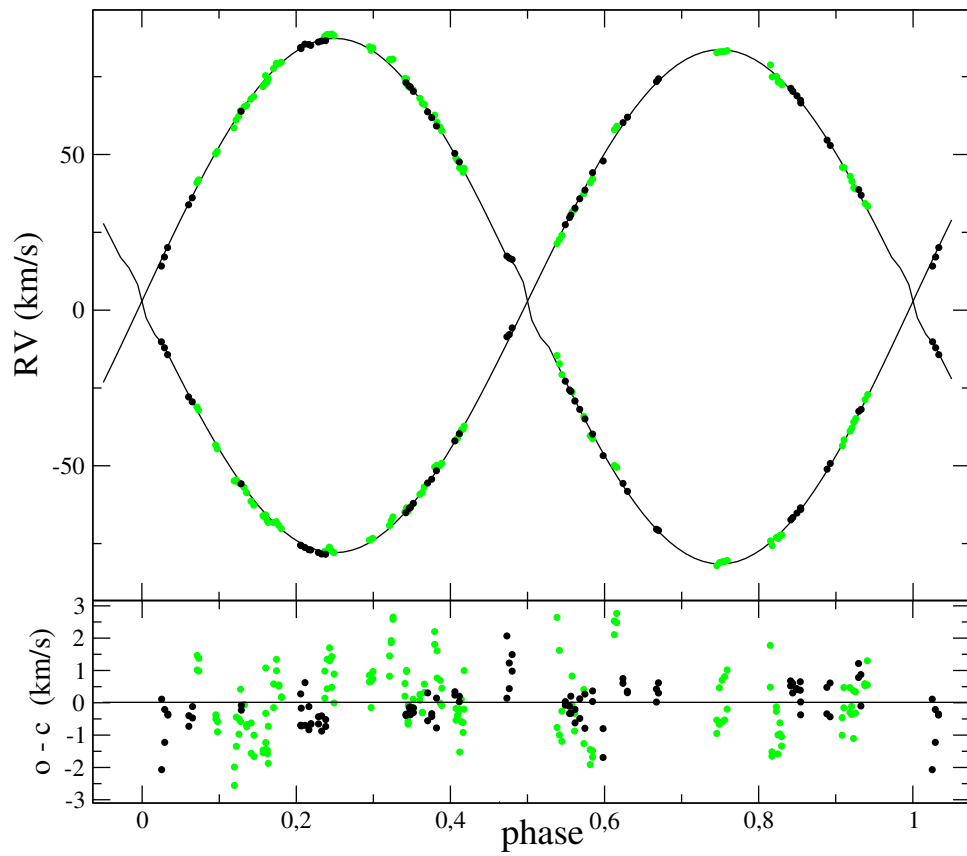


Fig. 5. Radial velocity curves of V2080 Cygni. Green dots present the DDO measurements shifted up with  $1.1 \text{ km s}^{-1}$ . Black dots present the measured PST1 velocities while the straight lines – synthetic RV curves based on the model listed in the one before last column of the Table 3.

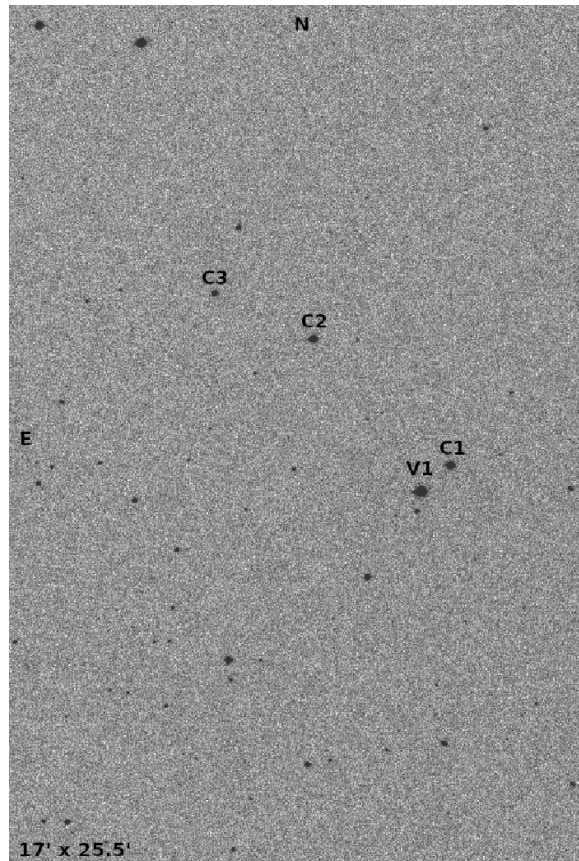


Fig. 6. Finding chart of V2080 Cyg. The variable is marked as V1. Positions of the three comparison stars C1, C2 and C3 are also shown. The field of view is about  $17.0' \times 25.5'$ . North is up, east is left.

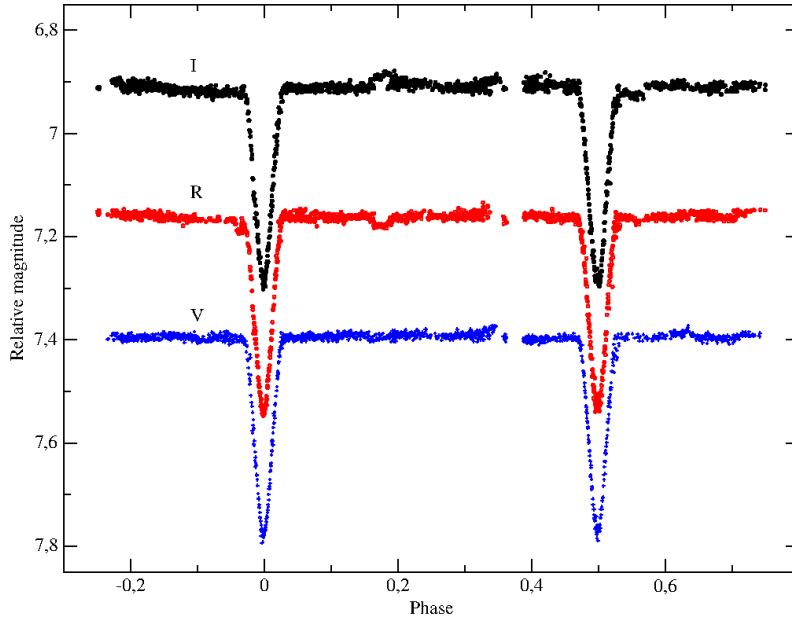


Fig. 7. The observed light curves in the I, R and V band passes for V2080 Cyg.

Dec= $+50^{\circ}14'04''.884$ , 8.98 mag in V filter), and C3 (RA= $19^h27^m16^s.991$ , Dec= $+50^{\circ}16'10''.986$ , 10.08 mag in V filter) were taken from the Tycho-2 Catalogue (Høg et al. 2000).

CCD frames were reduced with the *STARLINK*<sup>4</sup> package (Currie 2014). Corrections for bias, dark current and flat-field were applied and the aperture photometry was conducted.

In Fig. 7 we present the resulting light curves of V2080 Cyg in I, R and V filters. We used the value 4.9335 days as an orbital period to phase the data.

### 5.2. *O – C Diagrams for eclipses*

To check the stability of the orbital period and determine its value, the *O – C* analysis was conducted. First, we used the timings of 5 eclipses from our 2009-2011 observing season and the following ephemeris of the minima was derived:

$$\text{HJD}_{\min} = 2455094.3114(2) + 4.933550(2) \times E, \quad (1)$$

which gives the orbital period of  $P_{orb1} = 4.933550(2)$  days. The resulting *O – C* diagram for the moments of minima is shown in Fig. 8.

To obtain the best possible value of the orbital period we combined our 5 timings of eclipses from September 2009 - September 2011 observations, the Super-

<sup>4</sup>The Starlink software is currently supported by the East Asian Observatory

Table 4: The journal of the CCD observations of V2080 Cyg.

Year	Start date	End date	Number of nights	Exposure time [sec]	Number of frames	Filter
2009	September 7	November 21	19	10	6306	V
				8	7248	I
				6	9550	R
2010	October 17	October 31	5	10	1726	V
				8	2141	I
				6	3012	R
2011	May 23	October 1	17	10	5515	V
				8	6888	I
				6	8313	R
Total:	-	-	41	-	50699	-

WASP<sup>5</sup> June-July 2008 dataset, and the date presented in İbanoğlu et al. (2008). Based on this, we calculated the following ephemeris of the minima:

$$\text{HJD}_{\min} = 2455094.31027(9) + 4.9335701(4) \times E, \quad (2)$$

and this corresponds to the orbital period of  $P_{orb2} = 4.933701(4)$  days. In Fig. 9 we show the resulting  $O - C$  diagram for the moments of eclipses for 1998-2011 time span.

In Table 5 we present the timings of eclipses with errors, cycle numbers  $E$  and  $O - C$  values. As Type I and II are marked the primary and the secondary eclipses observed in V2080 Cyg, respectively.

The decreasing trend of the orbital period shown in Fig. 9 was confirmed by calculations of the second-order polynomial fit to the moments of minima. The following ephemeris was obtained:

$$\text{HJD}_{\min} = 2455094.31054(9) + 4.9335634(6) \times E - 2.7(2) \times 10^{-8} \times E^2. \quad (3)$$

In Fig. 9 the solid line corresponds to the ephemeris given by Eq. 3.

After this investigation, we suggest that the orbital period might have not been stable between August 1998 and September 2011 and it can be described by a decreasing trend with a rate of  $\dot{P} = -2.7(2) \times 10^{-8}$ . It should be noted that the observed change in the orbital period, presented in Fig. 9, was calculated based on the only one point of data from 1998 given by İbanoğlu et al. (2008). Hence, this time span of observations and the amount of available data are insufficient for any conclusive statement pertaining to the changes in the orbital period of V2080 Cyg.

---

<sup>5</sup><https://wasp.cerit-sc.cz>

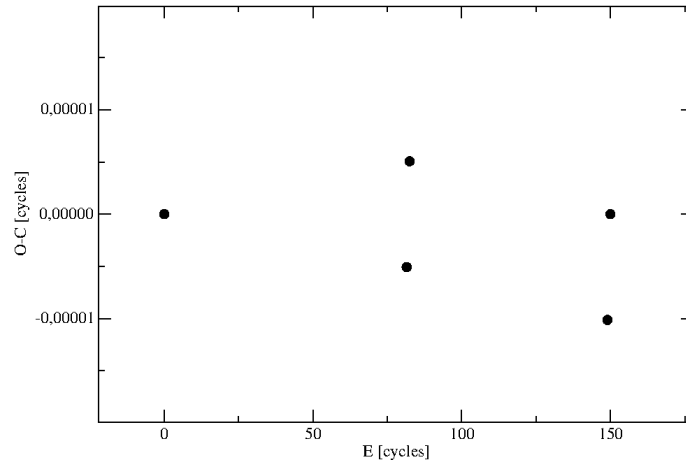


Fig. 8. The  $O-C$  diagram for the moments of eclipses observed in V2080 Cyg during our 2009-2011 campaign.

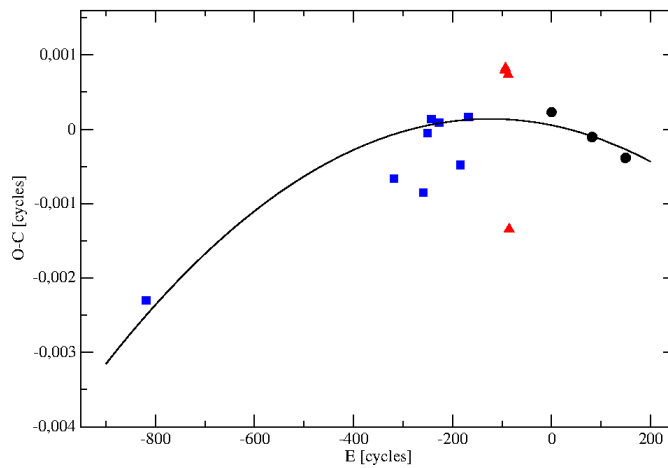


Fig. 9. The  $O-C$  diagram for the moments of eclipses in V2080 Cyg based on data collected between 1998 and 2011. Black circles represent our dataset, data taken from the SuperWASP are shown with red triangles, and blue squares correspond to data provided by İbanoğlu et al. (2008).

## 6. Conclusions

The investigated object V2080 Cyg is a well detached system, which provides possibility of precise measurements of absolute parameters. The star is bright and

Table 5: Times of minima in the light curves of V2080 Cyg observed from August 1998 until September 2011.

$E$	HJD <sub>min</sub> – 2450000	Error	$O - C$ [cycles]	Type	Reference
-819	1053.7050	-	-0.00230221	II	İbanoğlu et al. (2008)
-318	3525.4317	0.0008	-0.00066447	II	İbanoğlu et al. (2008)
-259	3816.5114	0.0006	-0.00085417	II	İbanoğlu et al. (2008)
-250.5	3858.4507	0.0003	-0.00005269	I	İbanoğlu et al. (2008)
-243	3895.4534	0.0001	0.00013467	II	İbanoğlu et al. (2008)
-227	3974.3903	0.0006	0.00089732	II	İbanoğlu et al. (2008)
-184	4186.5310	0.0003	-0.00048071	II	İbanoğlu et al. (2008)
-168	4265.4713	0.0006	0.00016353	II	İbanoğlu et al. (2008)
-94	4630.5586	0.0005	0.00079444	II	SuperWASP
-93	4635.4923	0.0008	0.00082077	II	SuperWASP
-87.5	4662.6265	0.0005	0.00073248	I	SuperWASP
-85.5	4672.4834	0.0006	-0.00134313	I	SuperWASP
0	5094.3114	0.0002	0.00022904	II	This work
81.5	5496.3957	0.0002	-0.00010807	I	This work
82.5	5501.3293	0.0003	-0.00010201	I	This work
149	5829.4103	0.0003	-0.00038814	II	This work
150	5834.3439	0.0004	-0.00038208	II	This work

the spectral lines of both components are clearly resolved. The lines of both components are blended only near the eclipse phases. The binary have three relatively bright visual companions however the GAIA proper motion and parallax results reveal that they are not connected with the EB as well as the dimmer background stars. We analysed our two radial velocity datasets obtaining a new mass determination based on a significantly higher number of measurements than the previous investigations. Comparing our and literature data we show that results depends on usage of different instruments and different measurement methods. The influence of the systematic errors on the obtained mass is about 1-2%. **Additionally we collected a photometric data and calculated a new times of minima. The analysis of the eclipse times show possible variation of the orbital period, which must be confirmed with a new measurements. Those variations could be related to the third body and the light time effect in the system.**

**Acknowledgements.** We would like to thank Slavek M. Rucinski and DDO staff for generous hospitality. In particular, our team wants to express appreciation to the observers Heide DeBond and Jim Thomson. We are grateful to our engineer

Roman Baranowski the cofounder of the Poznań Spectroscopic Telescope project. We thank the people who helped in observations: Agata Rożek, Krystian Kurzawa, Anna Przybyszewska and Adrian Kruszewski. WD, TK, KK and ASC were supported by the Polish grant KBN 1 P03D 025 29.

This work has made use of data from the European Space Agency (ESA) mission *Gaia* (<http://www.cosmos.esa.int/gaia>), processed by the *Gaia* Data Processing and Analysis Consortium (DPAC, <http://www.cosmos.esa.int/web/gaia/dpac/consortium>). Funding for the DPAC has been provided by national institutions, in particular the institutions participating in the *Gaia* Multilateral Agreement.

## REFERENCES

- Baranowski, R., Smolec, R., Dimitrov, W., et al. 2009, *MNRAS*, **396**, 4.  
Currie, M. J., Berry, D. S., Jenness, T., et al. 2014, *ASPC*, **485**, 391C.  
Dommanget, J., and Nys, O., 1994, *Communications de l'Observatoire Royal de Belgique*, **115**, .  
Gaia Collaboration Brown, A. G. A., Vallenari, A., Prusti, T., de Bruijne, J. H. J., Mignard, F., et al. 2016, *A&A*, **special Gaia volume**, .  
Høg, E., et al. 2000, *A&A*, **355L**, 27H.  
İbanoğlu, C. et al. 2008, *MNRAS*, **384**, 1.  
Kahraman Aliçavuş, F. and Aliçavuş, F. 2019, *MNRAS*, **488**, 4.  
Kurpińska-Winiarska, M., Oblak, E., Winiarski, M. and Kundera, T. 2000, *IBVS*, **4823**, 1-3.  
Lindgren, L., Lammers, U., Bastian, U., Hernández, J., Klioner, S., Hobbs, D., et al. 2016, *A&A*, **special Gaia volume**, .  
Mason, B. D., Wycoff, G. L., Hartkopf, W. I., Douglass, G. G., and Worley, C. E., 2001, *AJ*, **122**, 3466.  
Prša, A., and Zwitter, T., 2005, *ApJ*, **628**, 426.  
Slavek Rucinski 1992, *AJ*, **104**, 1968R.  
Slavek Rucinski 2002, *AJ*, **124**, 1746R.  
Wilson, R. E., Devinney, E. J., 1971, *ApJ*, **166**, 605.